How can the parameterization of a process-based model help us understand real tree-ring growth?

Ivan I. Tychkov[a,*], Irina V. Sviderskaya[a], Elena A. Babushkina [b], Margarita I. Popkova[a], Eugene A. Vaganov[a], Vladimir V. Shishov[a,c,*]

[a] Siberian Federal University, L. Prushinskoi st., 2, Krasnoyarsk, 660075, Russia

[b] Khakas Technical Institute, Siberian Federal University, Shetinkin str., 27, Abakan, 655017, Russia

[c] Le Studium Loire Valley Institute for Advanced Studies, 1 rue Duponloup, 45000 Orleans, France

[*] Corresponded authors: Ivan I. Tychkov E-mail: ivan.tychkov@gmail.com

Vladimir V. Shsihov E-mail: vlad.shishov@gmail.com

Author Contribution Statement: I.T., V.S., and E.V. designed research, I.T., M.P. and V.S. performed research, E.B. contributed actual chronology, I.T., V.S., I.S., and E.V. wrote the manuscript.

Key Message. This study shows great potential of the well-validated VS-Oscilloscope (a visual accurate parameterization of the VS-model) for assessment of spatial-temporal cambium phenology, which is illustrated based on the analysis of comprehensive datasets from central Siberia.

Abstract (253 words)

Tree-growth response to changing climate varies depending on tree species, forest type, and geographical region. Process-based models can help us better understand and anticipate these outcomes. To characterize growth sensitivity to different climate parameters, we applied the VS-Oscilloscope analytical package, as a precise visual parameterization tool of the Vaganov-Shashkin model, to two contrasting habitats: one with tree-ring growth limitation by soil moisture (in the southern part of central Siberia) and the another with temperature limitation (in the middle part of central Siberia). We speculate that specific parameter values of the Vaganov-Shashkin model and their variability under local conditions and species are the key to understand different physiological processes in conifers. According to the simulation results for the temperature-limited site, wider rings of *Picea obovata* can result from a longer growing season. However, for the soil moisture-limited site, the final sizes of the tree rings of *Pinus sylvestris* were not affected by the length of the growing season but were primarily defined by the intra-seasonal variations in soil moisture, even under cold conditions. For the two sites, we obtained a 20-day difference between the two phenological dates, in which the early date could be associated with cambial initiation and the late date with the appearance of the first enlarging cell. In the case of central Siberia, the time period was half that of the southern Siberia. Such differences could be explained by both geography and species-specific responses to phenology. To test this hypothesis, additional tree-ring and climatic data for contrasted habitats would be needed.

Keywords: process-based model, VS-oscilloscope, parameterization, growing season, climate signal, tree-ring seasonal variability

1. Introduction

One of the common dendroecological problems relates to understanding how different forest ecosystems may react to climate change (Hughes et al., 2011), which is especially important for highly forested regions worldwide, such as Siberia (Briffa et al., 2008; Bunn et al., 2013; Kirdyanov et al., 2012; Soja et al., 2007; Shishov et al., 2002; Tchebakova et al. 2011). Information about the relationship of climate and tree growth can be extracted with high-resolution and precise dating of tree rings due to their capability to fix environmental signals in tree-ring structure during the time of tree-ring formation (Schweingruber, 1988; Fritts et al., 1999; Vaganov et al., 2006). Well-developed globally distributed datasets of tree-ring parameters (International Tree-Ring Data Bank (ITRDB) ***http://www.ncdc.noaa.gov/paleo*** and a Russian database of tree-ring chronologies ***https://lib.ipae.uran.ru/dchrono/***) as well as daily climate database (NCDC's archive of global historical weather and climate data ***https://www.ncdc.noaa.gov/cdo-web/***) cover a large area of the forested territory of the planet, which includes hundreds of sites and climate stations from different climatic zones and locations. These datasets are actively used in dendroclimatological studies (e.g., Cook, Kairiukstis, 1990; Schweingruber et al., 1996; Hughes et al., 2011; Hellman et al., 2016). However, for dendroecological and tree physiological research (e.g., analyses of tree phenology, species plasticity, wood formation, etc.), more site-specific information is needed. Unfortunately, few of the data presented in the above-mentioned repositories include daily climatic observations from adjacent meteorological stations, not to mention the fact that there are no other long-term instrumental observations of any type of phenological or physiological processes of tree growth. Thus, there is yet no reliable answer regarding how exactly woody species from different ecosystems will respond to expected climatic changes at regional and global scales. Improvement of our understanding of tree-growth processes and accurate interpretations of climatic signals in tree rings, as determined by tree-ring parameters during the growing season, have recently become possible through the application of process-based

models. There are a number of such models, e.g., Biome3 (Haxeltine, Prentice, 1996), MAIDEN (Misson et al., 2004), CASTANEA (Dufrene et al., 2005), CAMBIUM (Drew et al., 2010), and PRYSM (Dee et al., 2015), which simulate tree-ring growth based on non-linear effects of environmental conditions and which avoid most of the limits related to the use of linear regression techniques in dendroecology (Fritts, 1976; Cook and Kairiukstis, 1990; Hughes, 2010). The process-based Vaganov-Shashkin model (VS-model) is one such model and describes tree-ring growth as the result of multivariate nonlinear biophysical processes, including effects of temperature, precipitation, and seasonal day length changes on tree-ring growth (Fritts et al., 1991; Vaganov et al., 2006, 2011; Guiot et al., 2014). The VS-model provides non-linear simulations of tree-ring growth for widely distributed coniferous species and has been used to obtain unique patterns of climate-growth relationships at both intra- and inter-annual scales in North America (Anchukaitis et al., 2012; Evans et al., 2006), Mediterranean region (Touchan et al., 2012), China (Shi et al., 2008; Zhang et al., 2016; Gou et al., 2013; He et al., 2017, 2018a, 2018b; Yang et al., 2017***)*** and Siberia (Vaganov et al., 2011; Shishov et al., 2016; Arzac et al., 2018). The deterministic VS-Lite forward model (VSL-model) is a simplified version of the VS-model and uses monthly temperature and precipitation as input data (Tolwinski-Ward et al., 2011, 2013). The transformation from daily to monthly resolution significantly reduced the number of model parameters needed. As a result, VS-Lite is widely used for spatial-temporal analyses of tree-ring growth responses to climate changes in different forest systems around the globe (Evans et al., 2013; Tolwinski-Ward, 2015; Breitenmoser et al., 2014; Lavergne et al., 2015; Mina et al., 2016; Tipton et al., 2016; Chen et al., 2017; Pompa-García et al., 2017; Sánchez-Salguero et al., 2017; Tumajer et al., 2017). However, this simplification of the original VS-model resulted in a loss of ability to estimate seasonal cell production and cell sizes.

As with most of the process-based models, the initial purpose of the VS-model was to describe variability of tree-ring radial growth, particularly tree-ring formation as related to climatic influence, and to determine principal factors limiting tree-ring growth. However, the VS-model is a complex tool that requires a considerable number of model parameters that should be re-estimated for each forest stand. This leads to problems of accurate model parameterization, namely estimations of "optimal" values of the model parameters necessary to guarantee: (1) the best fit to the observed tree-ring chronologies; (2) identification of the specific seasonal cell production and enlargement; (3) reasonable ecological interpretation in terms of processes involved in the model (Gaucherel et al., 2008; Shishov et al., 2016). The VS-Oscilloscope (Tychkov et al., 2012, 2015; Shishov et al., 2016) is an accurate parameterization tool of the model presented in this study, which shows potential to effectively resolve requirements #1 and 3 above.

In earlier studies, the parameters of the VS-model and their variability in contrasted habitats were not analyzed sufficiently in depth (Evans et al., 2006; 2013; Breitenmoser et al., 2014; Tolwinski-Ward et al., 2013; Mina et al., 2016), although they may play a determinant role in modelling of tree-ring growth in different environments (Shishov et al., 2016; Yang et al., 2017).

The recent application of the VS-Oscilloscope is focused on (1) the usage of adjusted VS-parameter values (with ecological interpretation) that provide the best fit to the actual tree-ring chronologies from climatically contrasted sites, and (2) the assessment of differences in the model parameters for contrasting environmental conditions. As a result, the model captures significant diversity in non-linear tree-ring growth responses that are climatically induced.

Following that purpose, we applied the VS-Oscilloscope to simulate tree-ring enlargement in spruce (*Picea obovata* Ledeb.) and pine (*Pinus sylvestris* L.) trees growing in differing environmental conditions. The two contrasting tree-growth habitats were: (1) the middle part of Central Siberia close to the settlement of Tura within the continuous permafrost zone, where temperature is a principal limiting factor of tree growth (Kirdyanov et al., 2013; Shishov et al., 2016), and (2) the forest-steppe zone of southern Siberia, in which soil moisture limits tree-ring growth (Babushkina et al., 2014, 2015; Knorre et al., 2010; Shah et al., 2015; Fonti, Babushkina, 2016). Special attention has been paid to determine the weights and importance of each climatic and plant-soil-related factor of the model for tree-ring formation during favorable (wide tree rings are formed) and unfavorable (narrow tree rings are formed) environmental conditions.

2. Materials and Methods

2.1. Study area and weather conditions

To the best of our knowledge there is no available data (published or not published) about the same tree species, or even a genus, with different limiting factors in diverse habitats for a vast territory of Siberia. For that reason two dendrochronological sites with spruce (*Picea obovata* Ledeb.) and pine (*Pinus sylvestris* L.) trees were chosen for analysis.

The site where tree-ring growth is limited by temperature (PlatPO) is located in the middle part of Central Siberia (64°17’ N, 100°13’ E, 610 m a.s.l.) (**Fig. 1**). The climate is continental with short and cool to mild summers and long winters. The mean annual air temperature is −9 °C, and the annual precipitation is 370 mm. To select the set of model parameters providing the best-fit model, daily weather records from the Tura meteorological station were used. Wood samples of spruce trees (*Picea obovata* Ledeb.) up to 276 years old were taken for the

144 analysis in a spruce-larch mixed stand with an admixture of birch (*Betula pubescens*)
145 (Shishov et al., 2016).

146 The MIN site, where growth is limited by moisture, is located in the Altai-Sayan region
147 (53°43' N, 91°50' E, 325 m a.s.l.) in a temperate climatic zone with a semi-arid cold climate
148 (Grigoryev, Budyko, 1960) (**Fig. 1**). The average annual temperature is approximately 1°C.
149 The average amount of precipitation per year is 330 mm, of which approximately 81-91%
150 falls within the period from April to October. The first half of the growing season is
151 characterized by a lack of atmospheric moisture (low ratio between the amounts of
152 precipitation and evaporation). At this site, *Betula pendula* Roth. and *Pinus sylvestris* L. trees
153 dominate in the sedge-grass-forb forest on sand dunes. We used a *Pinus sylvestris* ring-width
154 chronology and daily weather records from the Minusinsk station.

155 **2.2. Wood sampling, tree-ring width measurements, development of ring-width series**

156 The tree-ring chronology for the PlatPO site was obtained from 32 cores of 25 trees collected
157 in the autumn of 2009. The MIN tree-ring width chronology was built with 22 cores taken
158 from 19 trees in August of 2014. Tree-ring width (TRW) was measured with LINTAB 5.0 in
159 combination with the TSAP program (Rinntech, Heidelberg, Germany). The tree rings were
160 visually crossdated on wood cores, and the crossdating quality was verified using the
161 COFECHA program (Grissino-Mayer, 2001). To eliminate the influence of non-climatic
162 factors (e.g., age affects, abrupt changes caused by fires or defoliation caused by insects) on
163 tree radial growth, a 50%-variance cubic smoothing spline with a 2/3 cut-off time series
164 length was used as the detrending method. Autoregressive modeling was applied to remove
165 autocorrelations from the detrended time-series. Finally, the residual tree-ring chronology was
166 obtained using the bi-weight robust average procedure (Cook and Kairiukstis, 1990). The
167 climate-growth relationships were estimated *via* a Pearson correlation analysis (Cook and
168 Kairiukstis, 1990).

2.3. VS-model

The Vaganov–Shashkin simulation model is a process-based forward model that describes the formation of tree rings in relation to three environmental parameters: air temperature, soil moisture and solar irradiation. Here we provide a very brief description of the VS-model, but complete details can be found in Vaganov et al. (2006; 2011).

The input data for the model are daily records of mean temperature and total precipitation. Taking into consideration the amount of precipitation, intensity of transpiration depending on temperature and air relative humidity, and infiltration (Thornthwaite, Mather, 1955), the model calculates the moisture content in the soil for each day of the season. The values of daily solar irradiation coming from the upper atmosphere are determined by the latitude and day of year (Gates 1980).

For each *i*-day of the year, the model provides the integral rate of tree-ring growth $Gr(i)$ that is determined as the minimum of two partial growth rates: the growth rate that is dependent on the daily air temperature (Gr_T) and the partial growth rate that is dependent on daily soil moisture (Gr_W), multiplied by the value of growth rate influenced by daily solar irradiation (Gr_E) at the given latitude and on i^{th} day of the year:

$$Gr(i) = \min(Gr_T(i), Gr_W(i)) \cdot Gr_E(i) .$$

We consider the integral rate as a proxy estimate of the external component of tree-ring growth rate during the season. All the rates were determined in relative units within the range of zero to one. For each season, the ring-width indices, RWI, were calculated using the equation

$$RWI = \sum_{i=1}^{N} \frac{Gr(i)}{\overline{Gr}},$$

where *N* is the day count in the season, and $\overline{Gr}$ is the average growth rate over the calibration or verification period. The simulated ring-width indices were compared with the ring-width indices of the actual chronology for MIN.

To quantify the agreement between the simulated and actual ring-width series, we used Pearson correlation coefficient (R), the coefficient of synchronicity (S) (Huber, 1943; Shiyatov, 1986; Savva et. al., 2002), and the variance ratio (for more details, see Supplementary Material). The model variance should be not higher than the variance in the actual chronology because the VS–model describes the ring-width variability caused by climate factors.

2.4. Model parameterization procedure.

To obtain the combination of model parameters that provide the best fit of simulated tree-growth values with the actual tree-ring chronology, we used a specially designed application, the VS-Oscilloscope[1] (Shishov et al., 2016). The result of changing (decreasing/increasing) a value of the selected parameter is displayed on the graph chart of VS-Oscilloscope. It allows fits between simulated growth curves and the actual tree-ring chronologies to be visually evaluated. Moreover, quantitative estimations of their agreement such as Pearson correlation R, the coefficient of synchronicity S (Huber, 1943) and variance ratio between simulated and actual chronologies are re-calculated (for more details, see Supplementary Material). When using the VS-Oscilloscope, the user also monitors that the combination of parameter values is within the acceptable ecophysiological range (Rossi et al., 2013).

To validate the model results, the time spans of direct climate observations (A.D. 1934-2009 for MIN; A.D. 1950-2009 for PlatPO) were divided into two independent parts: calibration (A.D. 1960-2009 and A.D. 1970-2009 for the MIN and PlatPO sites, respectively) and

[1] The updated Lazarus Code of the VS-Oscilloscope and distributive package (CC BY SA license) can be downloaded from http://vs-genn.ru/downloads/.

verification (A.D. 1936-1959 and A.D. 1950-1969, respectively) periods. This is a standard technique used in dendrochronology to validate linear regression models (Cook and Kairiukstis, 1990).

2.5 Wide and narrow rings as indicators of favorable/unfavorable growing conditions

In the actual chronologies and corresponding simulated growth time series for both sites, we selected two groups of favorable (unfavorable) growing seasons (i.e., the years) when most of the corresponding wide (narrow) tree rings were formed. We defined wide rings as those whose ring-width indices exceed the mean value of the chronology by more than one standard deviation, whereas narrow ring-width indices are those that are at least one standard deviation below the mean value. Based on the described procedure, we selected (1) favorable growing seasons for the MIN site (1936, 1938, 1970, 1982, 1993, 1995, 1997, 2003, and 2006) and PlatPO site (1979, 2001, 2002, and 2005) when most of the wide rings were formed and (2) unfavorable growing seasons for the MIN site (1942, 1943, 1945, 1946, 1964, 1965, 1969, 1974, 1983, and 1998) and PlatPO site (1950, 1951, 1961, 1974, 1977, 1987, 1988, and 1989) when the narrow rings were formed.

3 Results

3.1 Model calibration and verification

Applying the VS-Oscilloscope parameter adjustment procedure (see Table S1), we obtained significant positive correlations between the actual tree-ring indices and simulated growth curves for both sites, i.e., for the (1) MIN site, Pearson's correlation coefficient $R = 0.71$ and coefficient of synchronicity S=80% ($p < 0.0001$, $n = 50$ years) for the calibration period 1960–2009 (**Fig. 2A**) and for (2) the PlatPO site, $R = 0.65$ and S=73% ($p < 0.0001$, $n = 40$) during the 1970-2009 period (**Fig. 2B**). The VS-model run with the same set of obtained parameters for the verification periods (MIN 1936–1959 and PlatPO 1950-1969) resulted in a simulated tree-ring growth curve characterized by good agreement with the actual tree-ring

chronology: R =0.53, S=70%, p <0.0001, and n=24 years for the MIN site (**Fig. 2A**) and R =0.5, S=80%, p <0.0001, and n=20 years for the PlatPO site (**Fig. 2B**).

3.2 Climate-growth correlations of actual and simulated chronologies

Correlation analysis between the actual and simulated tree-ring chronologies and monthly climate data was carried out during for a 13-month window from August of the previous year to August of the then current year over 1936-2009 and 1950-2009 for the MIN and PlatPO sites, respectively (**Fig. S1**). The actual and simulated chronologies demonstrate similar patterns in their relationships with monthly temperature and precipitation in both cases. MIN tree-ring growth is characterized by positive effects of precipitation in current May-July (Pearson correlation range: 0.33 to 0.52, $p<0.005$), negative effects of temperature during those months (-0.24 to -0.20, $p<0.05$), as well as positive effects of the previous year's November precipitation ($p<0.01$) (**Fig. S1A**). The tree-ring growth at the PlatPO site is significantly correlated with current-year June-July temperature (correlation range: 0.25 to 0.62, $p<0.05$), which affects the start of growing season (**Fig. S2B**). There are no significant correlations with previous-year temperature and precipitation.

3.3 Model parameter variations and agreement between the actual and simulated chronologies: importance of adjusting the parameters

As an example, we consider in detail how the variations in the values of the model parameters affected the agreement between the simulated and actual chronologies. In the VS-model, there are two related temperature parameters that determine the timing of tree-ring growth start, i.e., the minimum temperature for tree-ring growth T_{min} (^{o}C) and temperature sum for growth initiation T_{beg} (^{o}C). When the mean air temperature reaches T_{min}, the model starts to sum the mean daily temperatures until the sum for ten successive days equals T_{beg}, and on the next day, the tree-ring formation starts.

To show the influence of T_{min} and T_{beg} changes on the variability of modeled growth curve, we compared the tree-ring width obtained at different values of these parameters with the actual tree-ring chronology for the MIN site while the values of the other parameters were fixed (see Table S1). The value of T_{beg} was changed from 70 °C to 150 °C in 10 °C steps, and T_{min} – was changed from 1 °C to 10 °C in 1 °C steps.

When T_{min} was increased from 1 °C to 5 °C, the variances of the simulated growth time series did not change and equaled the variance of the actual chronology**.** The simulated variances were higher than the observed variance as T_{min} was varied between 6 and 10 °C. As T_{beg} was changed from 70 to 90 °C, the calculated variance was 5.2 times higher than that observed. Above that, the simulated variances decreased and became equal to the actual variance at T_{beg}=110 °C. The Pearson correlation values between the model and actual chronologies responded differently and were highest when T_{beg}=110±130 °C and T_{min}=1±5 °C (**Fig. 3A**). The coefficient of synchronism reached the maximum at T_{beg}= 120 °C and T_{min} =5 °C (**Fig. 3B**). Therefore, the maximum agreement between the model and actual chronologies occurred for T_{beg}=110 °C and T_{min} =5 °C (**Fig. 3**).

A similar sensitivity test was undertaken for other model parameters, and the most sensitive (influential) parameters are presented in Table S1. We defined the parameter as influential if the correlation and synchronicity coefficients varied more than 1% by changing the parameter values.

3.4 Analysis of intra-seasonal kinetics of tree-ring growth

The VS-model provides us the ability to estimate the duration of growing seasons, describe soil moisture kinetics and growth rate changes within the seasons, and determine which factor, air temperature or soil moisture, limits tree-ring growth on each day of the season.

For the MIN site, the best-fit model parameterization shows that all growing-season timing and duration values vary substantially (Table 1). The season duration varies from 105 to 158

days; the season can start as early as the end of April and as late as early June. However, most often the season begins in the middle of May and ceases in the middle of September, and the mean value of season duration is 130(±11) days. The time lag between DOYtmin (day of the year when the daily temperature reaches the T_{min} threshold) and DOYbeg (estimated start of the growing season) can vary from 9 to 64 days. The minimum temperature for growth, Tmin, is reached within the period from the middle of March to late April.

For the moisture-limited site, the longer season did not result in wider rings, as there are no relationships between the timing of the season start, end, and duration with the actual tree-ring indices (**Fig. S2A, Figs. S5A, B**). Moreover, by employing the ANOVA approach, we did not find any significant differences in the duration of growth seasons between years when wide and narrow rings were formed (Table 1, **Fig. S5A**). In both groups of selected rings/seasons, the patterns of soil moisture kinetics are very similar (**Figs. S3C, D**). Usually, the soil moisture reaches its highest values in late May to early June, and the lowest values occur in late June to middle July, which corresponds well to the regular summer droughts in the local environment. During the seasons when wide rings are formed, the soil moisture is always greater than during the seasons when narrow rings are formed (**Fig. 4**). The maximum values of air temperature usually occur in late June–early July (**Fig. S3A**). During growing seasons when wide rings were being formed, the soil moisture (**Fig. S3C**) as well as a partial growth rate depended on soil moisture Gr_W (**Fig. 4A**), and the integral growth rates Gr (**Fig. 4B**) were significantly higher than during the seasons when narrow rings were formed. The obtained results shown in the **Fig. 4** are confirmed by one-way ANOVA for the variabilities of Gr_W and Gr in wide and narrow rings (**Fig. S4A**). The mean values of Gr_W and Gr are significantly higher in the group of wide rings. This indicates the negative effects of high May-July temperature on tree-ring growth during the season (**Fig. S1A**). Higher air temperatures resulted in higher transpiration and decreased soil moisture (**Fig. 5).**

Regarding growth conditions at the temperature-limited PlatPO site, growing-season duration varies from 67 to 108 days, which is much less than for the MIN site. The mean duration of the growing season is 86(±10) days, and the season starts in early June and ends in late August (Table 1). The time-lag between DOYtmin and DOYbeg can vary from 6 to 62 days. The minimum temperature threshold for growth, Tmin, is reached within the period from the middle of March to early June.

According to simulation results, a wider tree ring will result from an earlier start and a longer duration of the growing season (**Fig. S2B**, **Figs. S5C, D**). Although the dates of the end of the growing seasons for wide and narrow rings are almost the same (**Fig. S5D**), the dates of the beginning of the growth seasons differ significantly (**Fig. S5C**).

The growing season for wide rings begins during the last week of May or in early June (152 ±7 days), and narrow rings start to grow in the middle or end of June (166±11 days) for PlatPO (Table 1). The average duration of the growing season for wide rings is approximately 94(±15) days and that for narrow rings is 80(±10) days.

The narrow rings were formed in the years when the temperature values (**Fig. S3B**) as well as corresponding partial growth rates depended on temperature Gr_T, and the integral growth rates Gr (**Figs. 4C, D**) are significantly lower in comparison with years when the wide rings were formed. According to the one-way ANOVA for the variability in the growth rates in the wide and narrow rings (**Fig. S4B**), the mean values of the Gr_T and Gr for wide rings are significantly higher. We noted that there is a significant difference in the soil moisture kinetics (**Fig. S3D**) and, as a result, in the partial growth rates dependent on soil moisture Gr_W. However, it does not affect the final sizes of tree rings because soil moisture is not a principle factor for tree-ring growth for PlatPO.

4. Discussion

In this study, we concentrated our attention on how the VS-parameter adjustment (parameterization) is important in the cases of two contrasting habitats. It was confirmed that the adjusted values of the model parameters depend not only on difference in local environmental conditions but also reflect the unique cambial phenology and physiology of different tree species (Shishov et al., 2016, Yang et al., 2017, He et al., 2018b). Moreover, the VS-model parameterization calculates year-to-year best-fitted variability of tree-ring width *via* calculations of the seasonal kinetics of tree-ring formation, and we have justification to consider the simulated kinetics of tree-ring seasonal growth to be an adequate representation of the actual kinetics of tree-ring seasonal growth and climate influence (Vaganov et al., 2011).

The choice of the two tree species was due to the fact that the tree growth was required to be definitely limited either by temperature or soil moisture in two sites.

Siberian spruce is one of the main species for Siberia. Due to its preferences to grow in moist places, *Picea obovata* is limited by temperature throughout the territory (Chytry et al., 2008, Lloyd et al., 2011). The climatic signal in tree rings becomes stronger by moving from favorable conditions of growth in the South (Babushkina et al., 2011) to less favorable in the North (Shishov et al., 2016)

Direct field observations for both species (*Pinus sylvestris* L. and *Picea obovata* Ledeb.) show that tree-ring growth starts almost at the same time in the conditions of southern Siberia (Babushkina et al., 2011). Thus, we can presume that differences in tree phenology between two sites might be influenced by climate rather than species difference, but this hypothesis still needs further investigation with additional field observations and data.

For these reasons we used Siberian spruce, *Picea obovata* and Scots pine, *Pinus sylvestris* growing in climatically contrasting habitats Central Siberia and Southern Siberia, accordingly,

and showing highly distinguishable responses to different limiting factors, temperature (Siberian spruce) and soil moisture (Scots pine).

Following the above-mentioned assumption that "the best fit values of model parameters should not conflict with field observations," the values of the obtained parameters can be considered. In the model, tree-ring growth starts when daily air temperature varies in the range of 5-9 °C, which is close to the temperature threshold value for conifer species provided by Rossi and co-authors (2007, 2013). This result agrees with the fact that Scots pine prefers light, sandy soils, although it also can be adapted to other types of soils where dry environments do not drastically affect growth (Lavergne et al., 2015; Levula et al., 2003; Linderholm, 2001). At the same time, Siberian spruce is a principal component of the boreal taiga of northern Russia, where it tends to dominate on shallow soils over permafrost and even on slightly deeper and better drained soils (Farjon, 2010, 2013; Shorohova et al., 2016).

The values for the lower and upper ends of the range of optimal temperatures (T_{opt1} and T_{opt2}) are in agreement with the average temperatures of summer months at both sites.

The adjusted soil moisture parameters show the model's ability to describe the adaptation of Scots pine and Siberian spruce trees to semi-arid and permafrost habitats, which is reflected in changing values of parameters relating growth rate with soil moisture and transpiration (W_{min}, W_{opt1}, W_{opt2}, W_{max}, C_2, and C_3) (Table S1). The values of the soil moisture parameters for the MIN site were relatively higher in comparison with the PlatPO parameters.

In this work, to understand better how VS-model parameterization can be interpreted, we used detailed information from previous studies in the research region, which provides an explanation of climate effects on tree-ring growth. Therefore, the significant correlation between the initial MIN chronology and climate for autumn months of the previous year (**Fig. S1A**) can be explained by the assumption that moisture is accumulated in the soil after the completion of the growing season. November is the period of first frosts and start of snow

386 cover, i.e., precipitation plays a protective role for trees in winter and can be considered as a
387 source of moisture for the next growing season. We did not observe such an autocorrelation
388 for the temperature-limited site PlatPO (**Fig. S1B**).

389 It was shown that temperature can play a role as a limiting factor during late spring- early
390 summer months even for the soil moisture-limited MIN site. First of all, temperature affects
391 the start and the end of the growing season in cold semi-arid conditions (Yang et al., 2017).
392 However, the most important fact is that increasing late spring temperatures can significantly
393 change soil surface evaporation rate. As a result, trees are under water stress (Fonti and
394 Babushkina, 2015), which can be confirmed by the formation of particularly narrow rings.

395 We especially note that the VS-model parameterization can provide important reliable
396 phenological information, e.g., the start and end of the growing seasons over several decades,
397 based on available daily climatic observations in a long-term historical context (see Table 1).
398 In practice, to obtain such information even for few years is a time consuming and complex
399 procedure (e.g., Antonova, Stasova, 1993; Peltola et al., 2002; Rossi et al., 2007, 2009, 2013).

400 Previously, it was shown that wider rings resulted from longer growing season durations due
401 to earlier start of the season (He et al., 2018b). We have confirmed that result in part. It was
402 correct in the case of the temperature-limited site PlatPO (**Figs. S5C, D**), i.e., wider rings can
403 result from longer growing seasons with higher rates of ring formation at the start and the
404 same rates for the season's remainder (**Figs. 4C, D**). The modeling results of the soil moisture-
405 limited site MIN show no significant detectable differences in the duration of the growing
406 seasons for formation of wide and narrow rings (Table 1, **Figs. S5A, B**), i.e., annual ring
407 widths that are positively correlated with seasonal cell production (Vaganov et al., 2006;
408 Popkova et al., 2018) are not determined by growing season duration. However, the value of
409 tree-ring width is mostly defined by the partial growth rate dependent on limiting factor (i.e.,

soil moisture for MIN), which is distinguished by intra-seasonal daily variations in temperature, precipitation and water lost due to transpiration and drainage in the middle part of growing season (**Fig. 4B**).

The best similarity between the modeled and actual chronologies is obtained if we determine the minimum temperature for growth as 5 (9) ºC and the effective temperature sum for the initiation of growth T_{beg} as 110 (100) over 10 days (Table S1) in the cases of the MIN and PlatPO sites, respectively. We observed the 20-day interval for PlatPO and the 40-day interval for MIN between the two dates (DOYbeg-DOYtmin) (Table 1) when the minimum temperature for growth (5-9 °C) is reached and when the first enlarging cell becomes visible in the cambium zone (or the emergence of first enlarging cambial derivatives) (Vaganov et al., 2006), that is when the 100 (110) degree-day sum over 10 days is reached. This result merits further research. One of the possible explanations is that reactivation of cambium starts when daily temperatures achieve 5-9º C. As the initial cycle length was evaluated to be 15–25 days, the beginning of the first xylem cell production (or appearance of the first enlarging cell) was evaluated to be 10-20 days. The sum of these two values gives us approximately 20-40 days between the two dates (Table 1). The 20-day difference in the value (DOYbeg-DOYtmin) between the two sites can be explained by the 70% decrease in growing-season length for the temperature-limited site PlatPO in comparison with the opposite at MIN (Table 1), which directly affects the corresponding shifts of the successive phases during xylogenesis (Rossi et al., 2013).

The issue of the initial temperature values and their correspondences with the beginning of cold year growing season, growth cessation and missing rings were discussed in the publications of Mann et al. (2012) and Anchukaitis et al. (2012). The discussed differences in the values of minimum temperature (5º instead of 10º C and vice versa) responsible for the start of xylogenesis can shift the growing season by more than 20 days to an early or late start

in the case of temperature-sensitive trees. In the PlatPO case, we obtained an approximately 20-day difference between initiation and the appearance of the first enlarging cell (see DOYbg – DOYtmin, Table 1). With the initiation of mother cells, it can take as many as 3-5 additional days to form a whole cambial zone. In the MIN case, the time cycle is even longer—up to 40 days (see Table 1). Therefore, the time difference between the dates of T_{min} and T_{beg} could be explained by the temporal delay between tree-ring growth initiation and the appearance of the first enlarging cell. The above-mentioned contradiction arises due to different definitions for the start of growing season. It could be the date of cambium initiation or the date of the appearance of the first enlarging cell.

5. Conclusions

We have shown that the parameterization of the VS-model is powerful tool to reliably explain the relationships between tree-ring growth, wood formation and cambium phenology over long periods of direct climate daily observation. The results obtained for the two contrasting habitats indicate that:

(1) the adjusted values of the model parameters depend not only on the differences in the local environmental conditions but also reflect the unique cambial phenology and physiology of the different tree species, *Pinus sylvestris* and *Picea obovata*;

(2) for the temperature-limited site, wider rings can result from a longer growing season with a higher rate of ring formation at the beginning of the season and the same rates for the rest of the season;

(3) in case of the soil moisture site, there are no significant differences in the duration of the growing seasons for the formation of wide and narrow rings, i.e. the width of annual rings is not determined by growing season duration but is significantly defined

458 by the intra-seasonal variation in the partial growth rate dependent on limiting factors
459 (i.e. soil moisture);

460 (4) two different time intervals have been estimated, i.e. 20-day interval for the PlatPO
461 site and a 40-day interval for the MIN site between the two dates (1) when the
462 minimum temperature for growth is reached (i.e. 5 and 9°C for MIN and PlatPO,
463 respectively) and (2) when the first enlarging cell becomes visible in the cambium
464 zone (or the emergence of first enlarging cambial derivatives), that is, when the 100
465 and 110 degree-day sum over 10 days is reached for PlatPO and MIN, respectively.
466 The 20-day difference in the values for the two sites could be explained by the 70%
467 decrease in growing season length for the temperature-limited site PlatPO in
468 comparison with that of MIN, which directly affects the corresponding shifts in the
469 successive phases during xylogenesis. To test this hypothesis, additional tree-ring and
470 climate data for other tree species and different habitats as well as direct xylogenesis
471 observations are needed.

472

473 **Acknowledgements**

474 We thank Dr. Thomas Melvin, Dr. Marina V. Fonti, Tatyana V. Kostyakova, Dr. Natalia I.
475 Kirichenko, two anonymous reviewers and communicating editor for providing valuable
476 constructive comments and suggestions during the preparation of the manuscript. We also
477 appreciate Dr. Alex Kirdyanov for the providing tree-ring measurements of PlatPO site.

478 **Funding**

479 I. T., M. P. and V. S. were supported by the Russian Science Foundation (project #14-14-
480 00219-P, process-based simulation, statistical analysis) and the Ministry of Education and

Science of the Russian Federation (project # 5.3508.2017/4.6, software development). V. S. appreciates the support by the Le Studium/Marie Skladowska-Curie Research Fellowship. M.P. and I.T. were supported by the Russian Foundation for Basic Research #18-34-00530 (data formatting and standardization). I. S., E. B., and E. V. funded by Russian Foundation for Basic Research, Government of Krasnoyarsk Territory, Krasnoyarsk Region Science and Technology Support Fund to the research project #17-44-240809/17 (data collection and measurements).

The authors declare that they have no conflict of interest.

References

Anchukaitis KJ, Breitenmoser P, Briffa KR, Buchwal A, Buntgen U, Cook ER, D'Arrigo RD, Esper J, Evans MN, Frank D, Grudd H, Gunnarson BE, Hughes MK, Kirdyanov AV, Körner C, Krusic PJ, Luckman B, Melvin TM, Salzer MW, Shashkin AV, Timmreck C, Vaganov EA, Wilson RJS (2012) Tree rings and volcanic cooling. Nature Geoscience 5: 836-837

Antonova GF, Stasova VV (1993) Effects of enviromental-factors on wood formation in Scots pine stems. Trees-Structure and Function 7: 214-219

Arzac A, Babushkina EA, Fonti P., Slobodchikova V, Sviderskaya IV, Vaganov EA (2018) Evidences of wider latewood in *Pinus sylvestris* from a forest-steppe of Southern Siberia. Dendrochronologia 49: 1–8. DOI:10.1016/j.dendro.2018.02.007

Babushkina EA, Knorre AA, Vaganov EA, Bryukhanova MV (2011) Transformation of the climatic response in the radial growth of trees, depending on the topoecological conditions of their growth. Geography and natural resources 1: 159-166 (in Russian)

503 Babushkina EA, Belokopytova LV (2014) Climatic signal in radial increment of conifers in
504 forest-steppe of southern Siberia and its dependence on local growing conditions. Russian
505 Journal of Ecology 45: 325-332
506 Babushkina EA, Vaganov EA, Belokopytova LV, Shishov VV, Grachev AM (2015)
507 Competitive strength effect in the climate response of Scots pine radial growth in south-
508 central Siberia forest-steppe. Tree-Ring Research 71: 106-117
509 Breitenmoser P, Bronnimann S, Frank D (2014) Forward modelling of tree-ring width and
510 comparison with a global network of tree-ring chronologies. Climate of the Past 10: 437-449
511 Briffa KR, Shishov VV, Melvin TM, Vaganov EA, Grudd H, Hantemirov RM, Eronen M,
512 Naurzbaev MM (2008) Trends in recent temperature and radial tree growth spanning 2000
513 years across northwest Eurasia. Philosophical Transactions of the Royal Society B-Biological
514 Sciences 363: 2271-2284
515 Bunn AG, Hughes MK, Kirdyanov AV, Losleben M, Shishov VV, Berner LT, Oltchev A,
516 Vaganov EA (2013) Comparing forest measurements from tree rings and a space-based index
517 of vegetation activity in Siberia. Environmental Research Letters 8. DOI:10.1088/1748-
518 9326/8/3/035034
519 Chen L, Huang JG, Stadt KJ, Comeau PG, Zhai LH, Dawson A, Alam SA (2017) Drought
520 explains variation in the radial growth of white spruce in western Canada. Agricultural and
521 Forest Meteorology 233: 133-142
522 Chytry M, Danihelka J, Kubesova S, Lustyk P, Ermakov N, Hajek M, Hajkova P, Kocı M,
523 Otypkova Z, Rolecek J, Reznıckova M, Smarda P, Valachovic M, Popov D, and Pisut I
524 (2008) Diversity of forest vegetation across a strong gradient of climatic continentality:
525 Western Sayan Mountains, southern Siberia. Plant Ecology. 196, 61–83. DOI
526 10.1007/s11258-007-9335-4

527 Cook ER, Kairiukstis LA (1990) Methods of dendrochronology: application in the
528 environmental science. Springer Science & Business Media, Kluwer Academic, Doredrecht,
529 DOI:10.1007/978-94-015-7879-0
530 Dee S, Emile-Geay J, Evans MN, Allam A, Steig EJ, Thompson DM (2015) PRYSM: An
531 open-source framework for PRoxY System Modeling, with applications to oxygen-isotope
532 systems. Journal of Advances in Modeling Earth Systems 7: 1220-1247
533 Drew DM, Downes GM, Battaglia M (2010) CAMBIUM, a process-based model of daily
534 xylem development in Eucalyptus. Journal of Theoretical Biology 264: 395-406
535 Dufrene E, Davi H, Francois C, le Maire G, Le Dantec V, Granier A (2005) Modelling carbon
536 and water cycles in a beech forest Part I: Model description and uncertainty analysis on
537 modelled NEE. Ecological Modelling 185: 407-436
538 Evans MN, Reichert BK, Kaplan A, Anchukaitis KJ, Vaganov EA, Hughes MK, Cane MA
539 (2006) A forward modeling approach to paleoclimatic interpretation of tree-ring data. Journal
540 of Geophysical Research-Biogeosciences 111. DOI:10.1029/2006JG000166
541 Evans MN, Tolwinski-Ward SE, Thompson DM, Anchukaitis KJ (2013) Applications of
542 proxy system modeling in high resolution paleoclimatology. Quaternary Science Reviews 76:
543 16-28
544 Farjon A (2010) A handbook of the world's conifers (2 vols.). Vol. 1. Brill, Netherlands. DOI:
545 10.1163/9789047430629
546 Farjon A (2013) Picea obovata. The IUCN Red List of Threatened Species 2013:
547 e.T42331A2973177. DOI:10.2305/IUCN.
548 Fonti P, Babushkina EA (2016) Tracheid anatomical responses to climate in a forest-steppe in
549 Southern Siberia. Dendrochronologia 39: 32-41
550 Fritts H (1976) Tree rings and climate. Academic Press (London and New York)

551 Fritts HC, Shashkin A, Downes GM (1999) A simulation model of conifer ring growth and
552 cell structure. In: Wimmer R, Vetter RE (eds) Tree-ring analysis: biological, methodological,
553 and environmental aspects. Wallingford, U.K.: CABI Publishing; 1999. 3-32
554 Fritts HC, Shashkin A, Downes GM. A simulation model of conifer ring growth and cell
555 structure. In: Wimmer, R.; Vetter, R.E. Eds., editors. Tree-ring analysis: biological,
556 methodological, and environmental aspects. Wallingford, U.K.: CABI Publishing; 1999. 3-32
557 Fritts HC, Vaganov EA, Sviderskaya IV, Shashkin AV (1991) Climatic variation and tree-ring
558 structure in conifers: empirical and mechanistic models of tree-ring width, number of cells,
559 cell size, cell-wall thickness and wood density. Climate Research 1: 97–116.
560 DOI:10.3354/cr001097
561 Gates DM (1980) Biophysical Ecology. Springer, Berlin, Heidelberg, New York, 611p.
562 Gaucherel C, Campillo F, Misson L, Guiot J, Boreux JJ (2008) Parameterization of a process-
563 based tree-growth model: Comparison of optimization, MCMC and Particle Filtering
564 algorithms. Environmental Modelling & Software 23: 1280-1288
565 Gou X, Zhou F, Zhang Y, Chen Q, Zhang J (2013) Forward modeling analysis of regional
566 scale tree-ring patterns around the northeastern Tibetan Plateau, Northwest China.
567 Biogeosciences Discuss. 10: 9969–9988. DOI:10.5194/bgd-10-9969-2013
568 Grigoryev AA, Budyko MA (1960) Classification of the Climates of the USSR. Soviet
569 Geography 1:3–24.
570 Grissino-Mayer HD (2001) Evaluating crossdating accuracy: a manual and tutorial for the
571 computer program COFECHA. Tree-Ring Research 57 (2):205-221.
572 Guiot J, Boucher E, Gea-Izquierdo G (2014) Process models and model-data fusion in
573 dendroecology. Frontiers in Ecology and Evolution 2: 52. DOI: 10.3389/fevo.2014.00052

574 Haxeltine A, Colin Prentice I (1996) BIOME3: An equilibrium terrestrial biosphere model
575 based on ecophysiological constraints, resource availability, and competition among plant
576 functional types. Global Biogeochemical Cycles 10: 693–709. DOI:10.1029/96GB02344
577 He MH, Shishov V, Kaparova N, Yang B, Brauning A, Griessinger J (2017) Process-based
578 modeling of tree-ring formation and its relationships with climate on the Tibetan Plateau.
579 Dendrochronologia 42: 31-41
580 He MH, Yang B, Shishov V, Rossi S, Brauning A, Ljungqvist FC, Griessinger J (2018a)
581 Projections for the changes in growing season length of tree-ring formation on the Tibetan
582 Plateau based on CMIP5 model simulations. International Journal of Biometeorology 62: 631-
583 641
584 He MH, Yang B, Shishov V, Rossi S, Brauning A, Ljungqvist FC, Griessinger J (2018b)
585 Relationships between wood formation and cambium phenology on the Tibetan Plateau
586 during 1960-2014. Forests 9: 86. DOI:10.3390/f9020086
587 Hellmann L, Agafonov L, Ljungqvist FC, Churakova O, Duthorn E, Esper J, Hulsmann L,
588 Kirdyanov AV, Moiseev P, Myglan VS, Nikolaev AN, Reinig F, Schweingruber FH,
589 Solomina O, Tegel W, Buntgen U (2016) Diverse growth trends and climate responses across
590 Eurasia's boreal forest. Environmental Research Letters 11. DOI:10.1088/1748-
591 9326/11/7/074021
592 Huber B (1943) Über die Sicherheit Jahrring – chronologischer Datierung. Holz als Roh- und
593 Werkst. **6**(10 -12): 263–268.
594 Hughes MK, Swetnam TW, & Diaz HF (Eds.). (2011) Dendroclimatology: progress and
595 prospects 11. Springer Science & Business Media. DOI:10.1007/978‐1‐4020‐5725‐0.
596 Jones PD, Bradley RS, & Jouzel J (Eds). (2013). Climatic variations and forcing mechanisms
597 of the last 2000 years (Vol. 41). Springer Science & Business Media.

598 Kirdyanov AV, Hagedorn F, Knorre AA, Fedotova EV, Vaganov EA, Naurzbaev MM,
599 Moiseev PA, Rigling A (2012) 20th century tree-line advance and vegetation changes along
600 an altitudinal transect in the Putorana Mountains, northern Siberia. Boreas 41: 56–67.
601 DOI:10.1111/j.1502-3885.2011.00214.x
602 Kirdyanov AV, Prokushkin AS, Tabakova MA (2013) Tree-ring growth of Gmelin larch
603 under contrasting local conditions in the north of Central Siberia. Dendrochronologia 31: 114-
604 119
605 Knorre AA, Siegwolf RTW, Saurer M, Sidorova OV, Vaganov EA, Kirdyanov AV (2010)
606 Twentieth century trends in tree ring stable isotopes ($\delta^{13}C$ and $\delta^{18}O$) of *Larix sibirica* under
607 dry conditions in the forest steppe in Siberia. Journal of Geophysical Research-
608 Biogeosciences 115. DOI:10.1029/2009JG000930
609 Lavergne A, Daux V, Villalba R, Barichivich J (2015) Temporal changes in climatic
610 limitation of tree-growth at upper treeline forests: Contrasted responses along the west-to-east
611 humidity gradient in Northern Patagonia. Dendrochronologia 36: 49-59
612 Levula J, Ilvesniemi H, Westman CJ (2003) Relation between soil properties and tree species
613 composition in a Scots pine-Norway spruce stand in southern Finland. Silva Fennica 37: 205-
614 218
615 Linderholm HW (2001) Climatic influence on Scots pine growth on dry and wet soils in the
616 central Scandinavian mountains, interpreted from tree-ring widths. Silva Fennica 35: 415-424
617 Mann ME, Fuentes JD, Rutherford S (2012) Underestimation of volcanic cooling in tree-ring-
618 based reconstructions of hemispheric temperatures. Nature Geoscience 5: 202-205
619 Lloyd AH, Bunn AG, Berner L (2011) A latitudinal gradient in tree growth response to
620 climate warming in the Siberian taiga. Global Change Biology 17: 1935-1945.
621 DOI**:** 10.1111/j.1365-2486.2010.02360.x

Mina M, Martin-Benito D, Bugmann H, Cailleret M (2016) Forward modeling of tree-ring width improves simulation of forest growth responses to drought. Agricultural and Forest Meteorology 221: 13-33

Misson L (2004) MAIDEN: a model for analyzing ecosystem processes in dendroecology. Canadian Journal of Forest Research 34: 874-887

Peltola H, Kilpelainen A, Kellomaki S (2002) Diameter growth of Scots pine (*Pinus sylvestris*) trees grown at elevated temperature and carbon dioxide concentration under boreal conditions. Tree Physiology 22: 963-972

Pompa-Garcia M, Sanchez-Salguero R, Camarero JJ (2017) Observed and projected impacts of climate on radial growth of three endangered conifers in northern Mexico indicate high vulnerability of drought-sensitive species from mesic habitats. Dendrochronologia 45: 145-155

Popkova MI, Vaganov EA, Shishov VV, Babushkina EA, Rossi S, Fonti MV, Fonti P (2018) Modeled tracheidograms disclose drought influence on *Pinus sylvestris* tree-rings structure from Siberian forest-steppe. Frontiers of Plant Science. DOI: 10.3389/fpls.2018.01144

Rossi S, Anfodillo T, Cufar K, Cuny HE, Deslauriers A, Fonti P, Frank D, Gricar J, Gruber A, King GM, Krause C, Morin H, Oberhuber W, Prislan P, Rathgeber CBK (2013) A meta-analysis of cambium phenology and growth: linear and non-linear patterns in conifers of the northern hemisphere. Annals of Botany 112: 1911-1920

Rossi S, Deslauriers A, Anfodillo T, Carraro V (2007) Evidence of threshold temperatures for xylogenesis in conifers at high altitudes. Oecologia 152: 1-12

Rossi S, Simard S, Rathgeber CBK, Deslauriers A, De Zan C (2009) Effects of a 20-day-long dry period on cambial and apical meristem growth in *Abies balsamea* seedlings. Trees-Structure and Function 23: 85-93

Sanchez-Salguero R, Camarero JJ, Carrer M, Gutierrez E, Alla AQ, Andreu-Hayles L, Hevia A, Koutavas A, Martinez-Sancho E, Nola P, Papadopoulos A, Pasho E, Toromani E, Carreira JA, Linares JC (2017) Climate extremes and predicted warming threaten Mediterranean Holocene firs forests refugia. Proceedings of the National Academy of Sciences of the United States of America 114: E10142-E10150

Savva Y, Schweingruber F, Milyutin L, Vaganov E (2002) Genetic and environmental signals in tree rings from different provenances of *Pinus sylvestris L.* planted in the southern taiga, central Siberia. Trees - Structure and Function 16: 313–324. DOI:10.1007/s00468-001-0136-4

Schweingruber FH (1988) Tree rings. Basics and applications of dendrochronology. Kluwer, Dordrecht.

Schweingruber FH & Briffa KR (1996). Tree-ring density networks for climate reconstruction. In: Jones PD, Bradley RS, & Jouzel J (eds) Climatic variations and forcing mechanisms of the last 2000 years. Springer, Berlin, Heidelberg: 43-66

Shah SK, Touchan R, Babushkina E, Shishov VV, Meko DM, Abramenko OV, Belokopytova LV, Hordo M, Jevsenak J, Kedziora W, Kostyakova TV, Moskwa A, Oleksiak Z, Omurova G, Ovchinnikov S, Sadeghpour M, Saikia A, Zsewastynowicz L, Sidenko T, Strantsov A, Tamkeviciute M, Tomusiak R, Tychkov I (2015) August to July precipitation from tree rings in the forest-steppe zone of central Siberia (Russia). Tree-Ring Research 71: 37-44

Shi J, Liu Y, Vaganov EA, Li J, Caim Q (2008) Statistical and process-based modeling analyses of tree growth response to climate in semi-arid area of north central China: A case study of *Pinus tabulaeformis*. Journal of Geophysical Research: Biogeosciences 113. DOI: 10.1029/2007JG000547.

Shishov VV, Tychkov, II, Popkova MI, Ilyin VA, Bryukhanova MV, Kirdyanov AV (2016) VS-oscilloscope: A new tool to parameterize tree radial growth based on climate conditions. Dendrochronologia 39: 42-50

671 Shishov VV, Vaganov EA, Hughes MK, Koretz MA (2002) The spatial variability of tree-
672 ring growth in Siberian region during the Last century. Doklady Earth Sciences 387 (5): 690-
673 694
674 Shiyatov SG (1986) Dendrochronology of upper timberline in Ural Mountains (in Russian).
675 Nauka, Moscow.
676 Shorohova E, Kapitsa E (2016) The decomposition rate of non-stem components of coarse
677 woody debris (CWD) in European boreal forests mainly depends on site moisture and tree
678 species. European Journal of Forest Research 135: 593-606
679 Soja AJ, Tchebakova NM, French NHF, Flannigan MD, Shugart HH, Stocks BJ, Sukhinin AI,
680 Parfenova EI, Chapin FS, Stackhouse PW (2007) Climate-induced boreal forest change:
681 Predictions versus current observations. Global and Planetary Change 56: 274-296
682 Tchebakova NM, Parfenova EI, Soja AJ (2011) Climate change and climate-induced hot spots
683 in forest shifts in central Siberia at the turn of the 21st century. Regional Environmental
684 Change 11(4): 817-827. DOI: 10.1007/s 10113-011-0210-4.
685 Thornthwaite CW, Mather JR (1955) The water balance. In: Climatology 1. Drexel Institute
686 of Technology, Philadelphia.
687 Tipton J, Hooten M, Pederson N, Tingley M, Bishop D (2016) Reconstruction of late
688 Holocene climate based on tree growth and mechanistic hierarchical models. Environmetrics
689 27: 42-54
690 Tolwinski-Ward SE, Anchukaitis KJ, Evans MN (2013) Bayesian parameter estimation and
691 interpretation for an intermediate model of tree-ring width. Climate of the Past 9: 1481-1493
692 Tolwinski-Ward SE, Evans MN, Hughes MK, Anchukaitis KJ (2011) An efficient forward
693 model of the climate controls on interannual variation in tree-ring width. Climate Dynamics
694 36: 2419-2439

695 Tolwinski-Ward SE, Tingley MP, Evans MN, Hughes MK, Nychka DW (2015) Probabilistic
696 reconstructions of local temperature and soil moisture from tree-ring data with potentially
697 time-varying climatic response. Climate Dynamics 44: 791-806
698 Touchan R, Shishov VV, Meko DM, Nouiri I, Grachev A (2012) Process based model sheds
699 light on climate sensitivity of Mediterranean tree-ring width. Biogeosciences 9: 965-972
700 Tumajer J, Altman J, Stepanek P, Treml V, Dolezal J, Cienciala E (2017) Increasing moisture
701 limitation of Norway spruce in Central Europe revealed by forward modelling of tree growth
702 in tree-ring network. Agricultural and Forest Meteorology 247: 56-64
703 Tychkov II, Koiupchenko IN, Ilyin VA, Shishov VV (2015) Visual parameterization of
704 Vaganov-Shashkin simulation model and its application in dendroecological research. Journal
705 of Siberian Federal University. Biology 8(4): 478-494 (In Russian)
706 Tychkov II, Leontyev AS, Shishov VV (2012) New algorithm of tree-ring growth model
707 parameterization: VS-oscilloscope and its application in dendroecology. Systems. Methods.
708 Technologies 4(16): 45-51. (in Russian)
709 Vaganov EA, Anchukaitis KJ, & Evans MN (2011) How well understood are the processes
710 that create dendroclimatic records? A mechanistic model of the climatic control on conifer
711 tree-ring growth dynamics. In: Hughes MK, Swetnam TW, Diaz HF (eds) Dendroclimatology
712 (pp. 37-75). Springer, Netherlands
713 Yang B, He MH, Shishov V, Tychkov I, Vaganov E, Rossi S, Ljungqvist FC, Brauning A,
714 Griessinger J (2017) New perspective on spring vegetation phenology and global climate
715 change based on Tibetan Plateau tree-ring data. Proceedings of the National Academy of
716 Sciences of the United States of America 114: 6966-6971
717 Zhang JZ, Gou XH, Zhang YX, Lu M, Xu XY, Zhang F, Liu WH, Gao LL (2016) Forward
718 modeling analyses of Qilian Juniper (*Sabina przewalskii*) growth in response to climate

719 factors in different regions of the Qilian Mountains, northwestern China. Trees-Structure and
720 Function 30: 175-188

721

722 Caption to the table

723 **Table 1.** The averaged simulated values of timing (DOY) for the two contrasted sites MIN
724 and PlatPO: DOYtmin is a date when the minimum temperature for tree growth T_{min} is
725 reached; DOYbeg is a date when the effective sum of temperature for growth initiation T_{beg} is
726 reached and the appearance of the first enlarging cell is observed; DOYstop is a date when the
727 cambial cell devision stops , DOYbeg - DOYtmin is a difference between two corresponding
728 dates, DOYstop - DOYbeg is a duration of cambial activity (growing season), ± 95%
729 confidence limits, in groups of wide and narrow rings.

730 Captions to figures

731 **Figure 1**. Map of study sites. Locations of the tree-ring sampled sites MIN and PlatPO
732 (circle) and the related meteorological station Minusinsk and Tura (triangle).

733 **Figure 2**. The actual tree-ring chronology (solid black line) and simulated one (solid grey
734 line) A) over 1936-2009 for MIN and B) over 1950-2009 for PlatPO. Dashed horizontal lines
735 is average index of tree-ring growth and standard deviation.

736 **Figure 3**. Estimated coefficient of correlation and synchronism between the actual and
737 simulated tree-ring chronologies at different values of parameters: T_{min} (A), T_{beg} (B).

738 **Figure 4.** The mean kinetics of partial growth rate on soil moisture during seasons when the
739 wide (black dashed curve) / narrow (grey solid curve) rings were being formed for MIN site
740 (A); the mean kinetics of integral growth rate during seasons when the wide (black dashed
741 curve) / narrow (grey solid curve) rings were being formed (B) for MIN site; the mean
742 kinetics of partial growth rate on temperature during seasons when the wide (black dashed
743 curve) / narrow (grey solid curve) rings were being formed for PlatPO site (A); the mean
744 kinetics of integral growth rate during seasons when the wide (black dashed curve) / narrow
745 (grey solid curve) rings were being formed (B) for PlatPO site. Vertical solid lines are
746 standard deviation.

747 **Figure 5.** The average partial growth rates on soil moisture $Gr_W(i)$, and temperature $Gr_T(i)$ for
748 1950–2009, for MIN (A) and PlatPO(B).

749 Tables

750 **Table 1.**

Group of rings	Number of rings in the group	DOYtmin	DOYbeg	DOYstop	DOYbeg– DOYtmin	DOYstop-DOYbeg
MIN site						
All rings (1936-2009)	74	98±2	138±2	268±2	39±3	130±3
Wide rings	9	99±7	137±7	270±3	37±7	133±8
Narrow rings	10	101±8	136±7	274±6	34±8	138±8
PlatPO site						
All rings (1950-2009)	60	143±10	160±8	246±7	17±12	86±10
Wide rings	4	136±5	152±7	246±7	15±7	94±15
Narrow rings	8	144±5	166±11	246±7	22±12	80±10

751

752

753 Figures

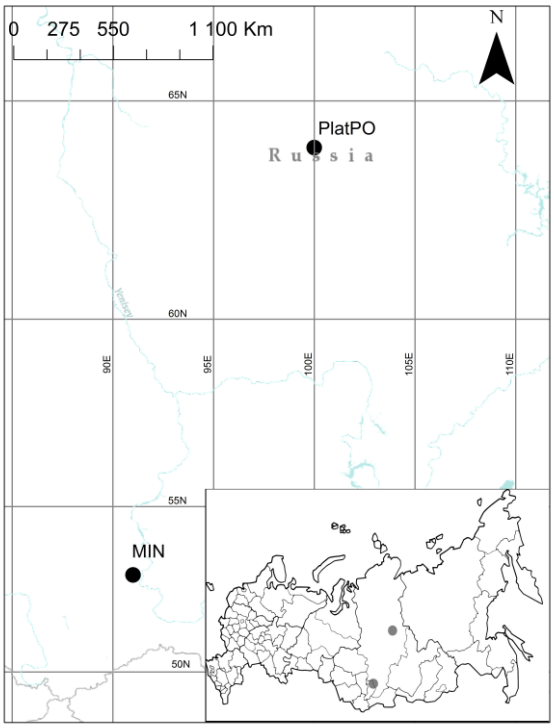

754

755 **Fig. 1**.

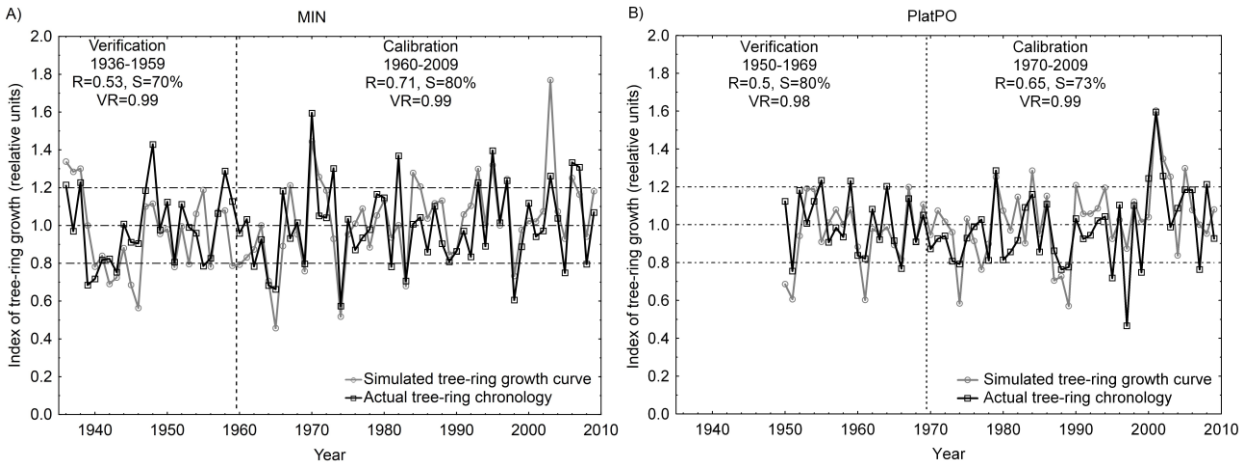

756

757 **Fig. 2**.

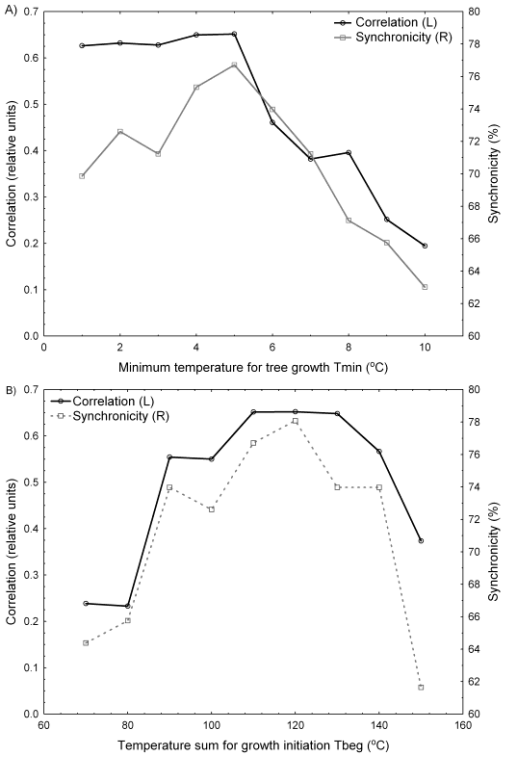

758

759 **Fig. 3**.

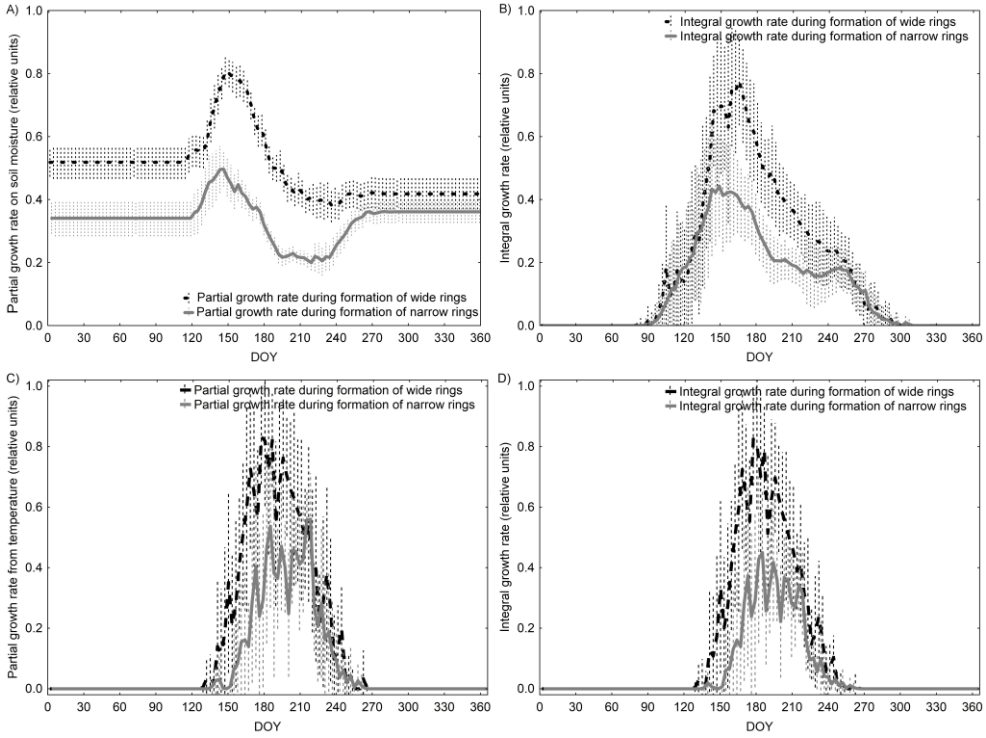

760

761 **Fig. 4.**

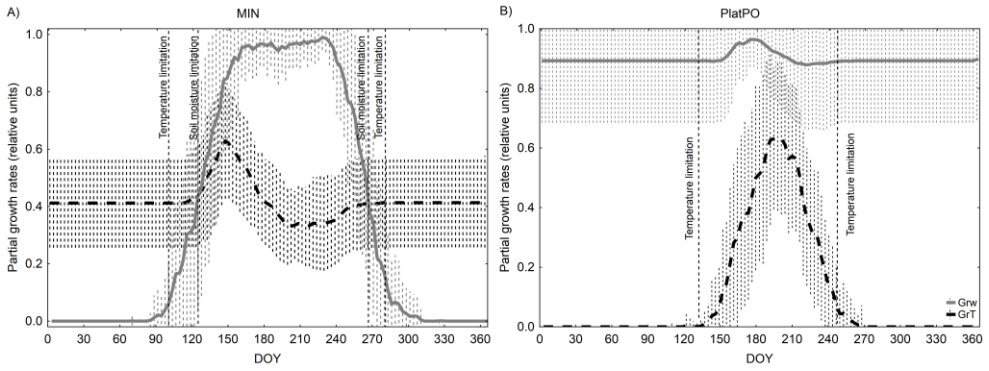

Fig. 5.

Supplementary material

How can the parameterization of a process-based model help us understand real tree-ring growth?

Ivan I. Tychkov[a,*], Irina V. Sviderskaya[a], Elena A. Babushkina [b], Margarita I. Popkova[a], Eugene A. Vaganov[a], Vladimir V. Shishov[a,c,*]

Analysis of similarity

For better assessment of similarity between simulated tree-ring growth curves and observed tree-ring chronologies, we used standard statistical estimations (e.g. Pearson correlation and coefficient of synchronicity), variance ratio and one-way ANOVA technique.

Usually, the coefficient of synchronicity, which is non-parametric statistics (Huber, 1943), is used for evaluation the coherence between two time series. We used it for evaluating the coherence between the simulated growth indices and the initial tree-ring chronologies (Shiyatov, 1986) based on the following equation:

$$S = \frac{n^{+} * 100}{n - 1},$$

where n^{+} is the number of segments from radial growth having the same tendency and n is the length of the compared period (in years) (Savva et. al., 2002).

Variance ratio *VR* is defined by the following equation:

$$VR = \frac{SD_m}{SD_{actual}},$$

where SD_m is the standard deviation of the simulated growth curve, SD_{actual} is the standard deviation of the actual tree-ring chronology. VR should not exceed one because simulated growth variance affected by climatic conditions is a part of the total variance of tree-ring chronology.

Tables

Table S1. Estimated VS-model parameters by the VS-oscilloscope**.**

Parameters	Description	MIN	PlatPO
T_{min}	Minimum temperature for tree growth (°C)	5	9
T_{opt1}	Lower end of range of optimal temperatures (°C)	13	22
T_{opt2}	Upper end of range of optimal temperatures (°C)	22	28
T_{max}	Maximum temperature for tree growth (°C)	32	33
W_{min}	Minimum soil moisture for tree growth, relative to saturated soil (v/vs)	0.0775	0.06
W_{opt1}	Lower end of range of optimal soil moistures (v/vs)	0.25	0.175
W_{opt2}	Upper end of range of optimal soil moistures (v/vs)	0.375	0.325
W_{max}	Maximum soil moisture for tree growth (v/vs)	0.45	0.575
W_0	Initial soil moisture (v/vs)	0.15	0.175
T_{beg}	Temperature sum for initiation of growth (°C)	110	100
t_{beg}	Time period for temperature sum (days)	10	10
l_r	Depth of root system (mm)	500	500
P_{max}	Maximum daily precipitation for saturated soil (mm/day)	40	40
C_1	Fraction of precip. penetrating soil (not caught by crown) (rel. unit)	0.5	0.43
C_2	First coefficient for calculation of transpiration (mm/day)	0.3075	0.18
C_3	Second coefficient for calculation of transpiration (mm/day)	0.11	0.125
Λ	Coefficient for water drainage from soil (rel. unit)	0.005	0.005
V_{cr}	Critical growth rate	0.04	0.01

Figures

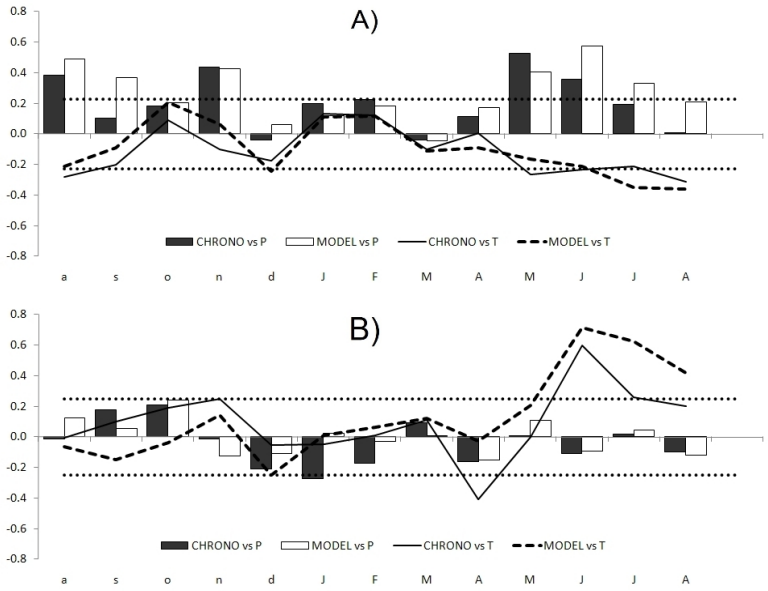

Figure S1. Correlations of actual tree-ring chronology and simulated one with monthly precipitation (columns) and temperature (lines) for MIN site (A) and for PlatPO site (B). Correlations were calculated from August of the previous year to August of current year. Horizontal dashed lines show significant limits of correlation**.**

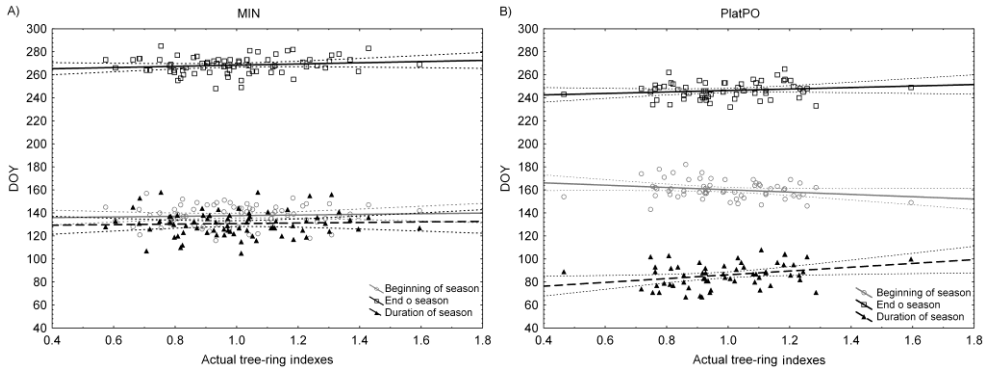

Figure S2. The simulated timing of the growth start (circles), end (squares), and season duration (triangles) *versa* the actual ring-width indices for MIN site (A) and for PlatPO site (B). Grey solid, dark solid, dashed black lines are regression lines obtained for the start, end and duration respectively. Dashed grey lines are 95%-confidence limits.

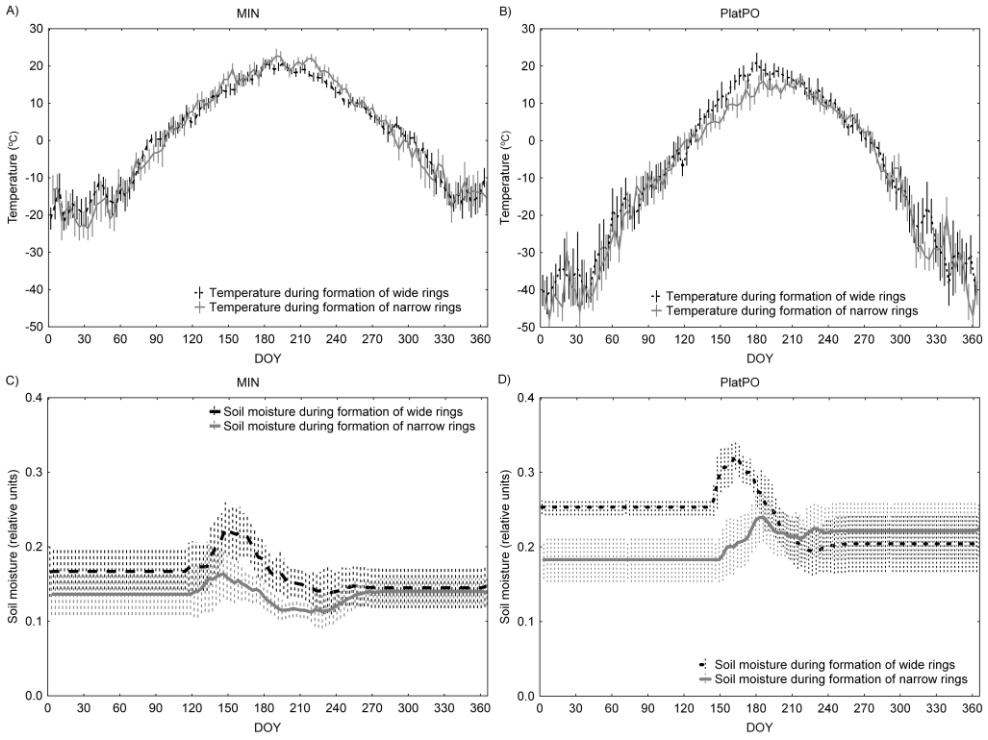

Figure S3. The mean variation of temperature for MIN site (A) and for PlatPO site (B) and soil moisture for MIN (C) and PlatPO (D) during seasons when the wide (black dashed curve) / narrow (grey solid curve) rings were being formed.

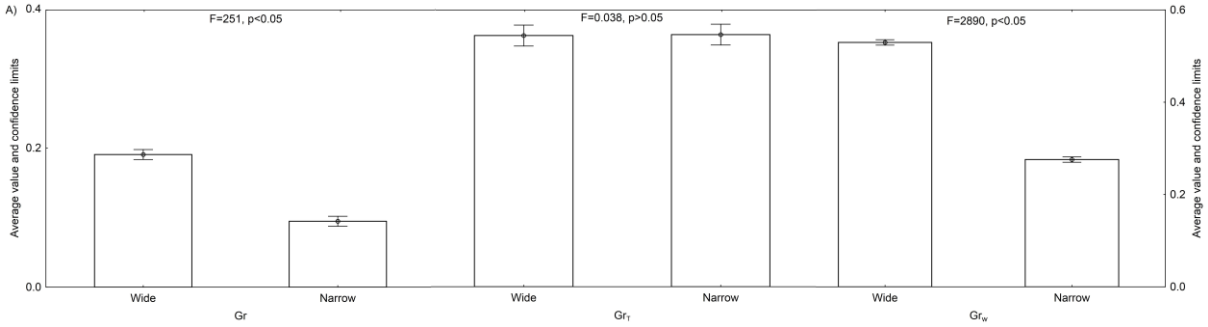

Figure S4. One-way ANOVA for groups of wide and narrow rings on integral growth rate Gr (left Y-axis), partial growth rate on temperature Gr_T (left Y-axis) and partial growth rate on soil moisture Gr_w (right Y-axis) for MIN (A) and PlatPO(B).

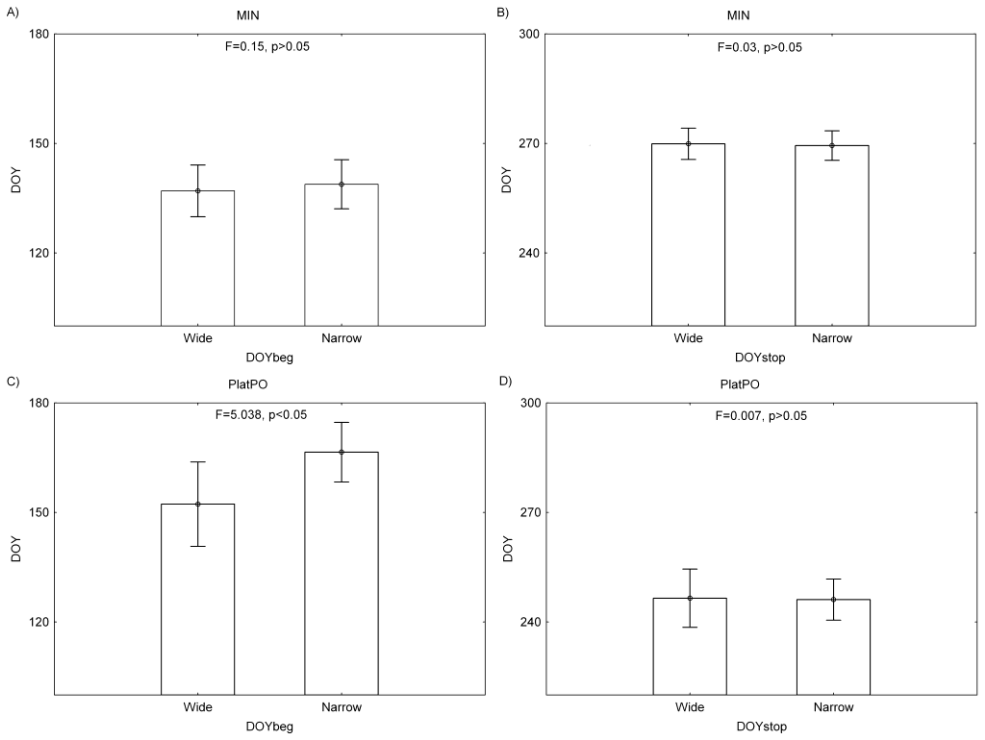

Figure S5. One-way ANOVA for groups of wide and narrow rings on start (A) and end (B) of growing season for MIN site; one-way ANOVA for groups of wide and narrow rings on start (C) and end (D) of growing season for PlatPO site